D. P. Kennedy

P. C. Murley

W. Kleinfelder

On the Measurement of Impurity Atom Distributions in Silicon by the Differential Capacitance Technique*

Abstract: A mathematical analysis is presented on the measurement of an impurity atom distribution in silicon by the differential capacitance technique. This analysis shows some inherent errors that can arise when the technique is applied to material containing a small impurity atom density. An important conclusion is that the differential capacitance measurement establishes the distribution of majority carriers, rather than the distribution of impurity atoms; therefore this measurement technique is applicable only in regions of semiconductor material exhibiting charge neutrality.

Introduction

The measurement of impurity atom distributions in semiconductor material is important both in fundamental investigations and in the design and development of semiconductor devices. A method frequently used to obtain such information is the differential capacitance technique. 1—4 This technique involves the use of a reversebiased abrupt asymmetrical p—n junction, or a similar structure, suitably located so that its space-charge layer penetrates into the region of semiconductor material under investigation. Because the electrical properties of an abrupt p—n junction are well understood, the measured differential capacitance of this test junction (throughout a range of reverse biasing voltage) can be used to quantitatively establish the impurity atom distribution within the semiconductor material.

An inherent experimental limitation of this technique results from avalanche mechanisms within the space-charge layer of the test junction. Avalanche breakdown limits the maximum voltage that can be applied to the test junction, and hence the maximum distance over which a given junction can be used to establish an impurity atom distribution; therefore this experimental method has only

At comparatively large values of impurity atom density, several different methods exist for determining the impurity atom distribution in a given sample of semiconductor material. By direct comparison, substantial agreement can be shown between the impurity profile established by differential capacitance measurements and by other methods. In contrast, at very small values of impurity atom density there is no direct experimental method for verifying the accuracy of an impurity atom profile obtained from differential capacitance measurements. Therefore the need for a rigorous mathematical investigation of this topic is apparent.

The material presented here results from a one-dimensional solution of the ambipolar diffusion equations for holes and electrons in semiconductor material. These mathematical equations are solved for an analytical model that approximates the differential capacitance experiment for measuring an impurity atom distribution. Briefly, the analytical model is composed of a region of semiconductor material containing a prescribed impurity atom distribution; this region is bounded at one end by a test junction

limited applicability in an investigation of material containing a large impurity atom density. As a result there is a tendency to use the differential capacitance technique in investigations of "low-doped" semiconductor material, and to use other techniques (for example, radio tracer methods) for material containing a large impurity atom density.

^{*} The analysis presented in this paper was supported in part by the Air Force Cambridge Research Laboratories, Office of Aerospace Research, under Contract F19(628)-CO116, Project 6300.

The authors are located at the IBM Components Division laboratories, E. Fishkill, New York.

(either an asymmetrical abrupt p-n junction or a Schottky barrier) and at the other end by an ohmic contact. A difterential capacitance measurement is mathematically approximated by applying to this analytical model a prescribed reverse biasing voltage (between the test junction and the ohmic contact) and calculating the resulting electrical capacitance. In this fashion, the test junction capacitance can be established for a sequence of reverse biasing voltages comparable to those used in a differential capacitance measurement of the impurity profile in a semiconductor.

This mathematical method has been used to calculate the capacitance-vs.-voltage charactersitics that would be obtained from differential capacitance measurements upon semiconductor material containing a prescribed impurity atom distribution. From this calculated capacitance information, in conjunction with conventional equations relating the impurity atom distribution to the measured capacitance, a comparison was made between the impurity atom distribution that would be established by differential capacitance measurements and the impurity atom distribution used in the analytical model. In situations where a difference was observed between the differential capacitance inferred profile and that of the model, a study was made to determine the source of difference. Thereby, this investigation has provided understanding of some inherent limitations of the differential capacitance technique; a discussion of these limitations is presented here.

List of definitions

- C Electrical capacitance
- D_n Diffusion constant for electrons
- D_n Diffusion constant for holes
- E Electric field
- J_n Electric current density due to electrons
- J_p Electric current density due to holes
- J_T Total electric current density
- N Ionized impurity atom density
- \mathfrak{R}_n Recombination rate for electrons
- \mathfrak{R}_n Recombination rate for holes
- V_j Total junction voltage
- W Electrostatic energy
- i Electric current
- ℓ Length of structure under investigation
- n Mobile electron density
- p Mobile hole density
- q Electron charge
- t Time
- ϵ_0 Permittivity of free space
- κ Dielectric constant
- $\mu_n D_n q/kT$
- $\mu_p D_p q/kT$
- Ψ Electrostatic potential

Mathemetical methods

In a homogeneous semiconductor, the hole and electron distributions [p(x)] and n(x) are described by the equations:

(a)
$$\frac{d^2\Psi}{dx^2} = -\frac{q}{\kappa\epsilon_0} \left[N(x) - n(x) + p(x) \right],$$

(b)
$$J_p = -q D_p \frac{dp}{dx} - q \mu_p p \frac{d\Psi}{dx},$$

(c)
$$J_n = q D_n \frac{dn}{dr} - q \mu_n n \frac{d\Psi}{dr}, \qquad (1)$$

(d)
$$0 = \Re_p(x) - \frac{1}{a} \frac{dJ_p}{dx},$$

(e)
$$0 = \Re_n(x) - \frac{1}{q} \frac{dJ_n}{dx},$$

$$(f) J_T = J_p + J_n.$$

Equation (1a) is Poisson's equation, which relates the divergence of the electric field to the total electric charge due to both mobile charge carriers and ionized impurity atoms. Throughout the present investigation, a wide selection of different impurity atom distributions was used in the mathematical model; these distributions will be discussed individually.

Equations (1b) and (1c) give the electric current densities within a semiconductor arising from the transport of mobile holes and electrons. They express the dependency of the electric current components $(J_p \text{ and } J_n)$ upon the concentration gradients of holes and electrons, the mobility of these charge carriers, and the electrostatic potential gradient within a semiconductor.

Equations (1d) and (1e) are the continuity equations for holes and electrons that are assumed to exhibit an unspecified recombination/generation mechanism. It has been a general practice in most applications of Eqs. (1) to adopt the recombination/generation mechanisms outlined in the Shockley-Read theory. Throughout the present investigation a simplification has been used for these equations which makes it unnecessary to introduce mechanisms attributable to minority carriers.

Equation (1f) states that the total electric current density is the algebraic sum of electric current due to both holes and electrons.

The equations listed in (1) can be combined into three simultaneous non-linear differential equations in three variables: electrostatic potential, mobile hole concentration, and mobile electron concentration. A rigorous mathematical analysis of this problem requires the simultaneous solution of these three equations, subject to the constraints imposed by both the geometrical and physical properties of the problem.

The analysis presented here results from a computer program developed for the one-dimensional simultaneous solution of these equations. In this computer program three nodal arrays are used to approximate the structure under investigation. These nodal arrays are individually composed of approximately 120 spatial locations that are suitably distributed to provide the required computational accuracy. The applicable differential equations are used in their finite-difference form, and simultaneous solutions are obtained for these three arrays by using relaxation methods.⁷⁻¹¹

A typical analytical model for which Eqs. (1) are solved is shown in Fig. 1. In this model the sample of semiconductor material is assumed to contain a prescribed impurity atom distribution. One end of this model is bounded by an ohmic contact, and the opposite end by a Schottky barrier type of rectifying contact.¹² The application of a reverse biasing voltage between the rectifying contact and the ohmic contact produces a space-charge layer that penetrates into the region of semiconductor material under investigation.

Each solution of Eqs. (1) yields the electric field distribution E(x) within the model shown in Fig. 1. From this field distribution, the associated electrostatic energy W is given by 13,14

$$W = \frac{\kappa \epsilon_0}{2} \int_0^1 E^2 dx \ . \tag{2}$$

In this analysis an electrostatic energy calculation is completed for each assumed value of biasing voltage; thereafter graphical means are used to determine the associated electrical capacitance,

$$C = \frac{1}{V} \frac{dW}{dV}. (3)$$

In this fashion a mathematical determination is made of the capacitance-vs.-voltage characeristic that would be obtained from laboratory measurements upon the prescribed sample of semiconductor material.

In an attempt to reduce the computer time for this investigation, a comparison was made between two forms of the calculated differential capacitance of this semiconductor structure; first, when the mechanisms attributable to minority carriers were included and second, when the minority carrier density was assumed to be zero. In no case was a significant difference observed when the influence of minority carriers was neglected. For this reason, the information presented here has been obtained from simplified solutions of (1) in which the minority carrier density is assumed to be zero.

The differential capacitance technique

The differential capacitance technique for profiling semiconductor material arises from the depletion layer theory of an abrupt asymmetrical p-n junction. A fundamental property of this junction is that one side is doped to an

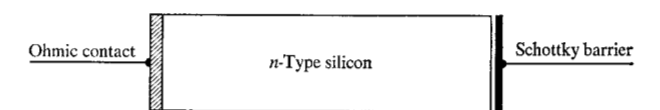


Figure 1 Analytical model used in this investigation.

impurity atom density which is several orders of magnitude greater than the other side; the junction space-charge layer thus extends much further into the region of small doping than into the region of large doping. Furthermore, this differential capacitance technique is based upon an assumption that the space-charge region in the low-doped side exhibits the physical simplifications used by Shockley in his development of the depletion layer theory of p—n junction operation. ¹⁵

From this depletion layer theory it has been shown² that the impurity atom density at the space-charge layer edge of an asymmetrical abrupt p-n junction (on the low-doped side) is given by

$$N(x) = -\frac{C^3}{g\kappa\epsilon_0} \left(\frac{dC}{dV}\right)^{-1}.$$
 (4)

Equation (4), in conjunction with a traditional expression for the electrical capacitance of p-n junction,

$$C = \frac{\kappa \epsilon_0}{x} \,, \tag{5}$$

is conventionally used in differential capacitance measurements of the impurity atom distribution in semiconductor material. In Eq. (5), $\kappa\epsilon_0$ is the permittivity of the semiconductor material, and x is the space-charge layer width.

It will be shown in this paper that Eq. (4) is only applicable to semiconductor material exhibiting charge neutrality. This conclusion has been derived from a series of computational experiments using the analytical model illustrated in Fig. 1. In these experiments a prescribed impurity atom distribution is assumed within this analytical model, and a series of calculations is performed [using Eqs. (1), (2), and (3)] to establish capacitance-vs.-voltage information one would obtain from differential capacitance measurements upon a sample of semiconductor material containing this same impurity atom distribution. Thereafter Eqs. (4) and (5) are used to determine the impurity atom distribution inferred by these capacitance calculations. Thereby a direct comparison is obtained between an impurity atom distribution used within the analytical model and the impurity atom distribution that would be inferred from differential capacitance measurements upon semiconductor material containing this same impurity atom distribution. At small values of impurity atom density, these impurity atom distributions (the capacitance-inferred distribution and the distribution used in the analytical model) were seldom in agreement. To understand the source of this difficulty a study was made of the approximations and simplifications used in the development of Eq. (4). This study has established some inherent limitations associated with the differential capacitance technique for measuring the impurity atom distribution in semiconductor material.

The small-signal capacitance of a reverse biased p-n junction arises from the electrostatic charge circulating within its external biasing circuit, due to an incremental change of applied biasing voltage,

$$C(V_j) = \frac{1}{dV} \int_0^\infty i(t)dt \bigg|_{V_j}. \tag{6}$$

For an asymmetrical abrupt p-n junction the magnitude of this electrostatic charge is established by the quantity of mobile electrons either removed or added to the low-doped material (assuming this material is n-type), due to a small change of space-charge layer width. Leaving out any specific reference to the junction biasing voltage, this quantity of mobile electrons is given by n(x)dx, where n(x) is the local density of mobile electrons at the space-charge layer edge and x is the space-charge layer width. Therefore the electrical capacitance of this p-n junction (per unit area) is given by

$$C = \frac{1}{dV} \int_0^\infty i(t)dt = q \, n(x) \, \frac{dx}{dV} \tag{7}$$

From Eqs. (5) and (7) we obtain

$$n(x) = -\frac{C^3}{q\kappa\epsilon_0} \left(\frac{dC}{dV}\right)^{-1}, \qquad (8)$$

where C is the differential capacitance of a test junction that is measured at a given reverse biasing voltage. Equation (8) represents our modified form of Eq. (4); this equation shows that differential capacitance measurements establish the majority carrier distribution in a semiconductor, not the impurity atom distribution.

It should be noted that Eqs. (4) and (8) are in quantitative agreement when applied to charge-neutral semiconductor material [since n(x) = N(x)]. For this reason differential capacitance measurements provide an important means to establish the impurity atom distribution in this particular type of semiconductor material. In contrast, differential capacitance measurements are of little value when applied to semiconductor material containing a substantial electrostatic charge; such measurements can produce a density distribution that is orders of magnitude larger (or smaller) than the impurity atom distribution. These conclusions have been verified by the previously described computational experiments.

Equation (7) is based upon an assumption that the p-n junction ideally satisfies the mechanisms of operation outlined in Shockley's depletion layer theory. In this theory the p-n junction space-charge layer is assumed to be depleted of mobile charge carriers, and to terminate in a discontinuous fashion. Because these idealizations cannot always be taken for granted, the lack of idealization of the test junction space-charge layer will be considered a possible source of error.

In an asymmetrical abrupt p-n junction, it can be shown¹⁶ that at potential equilibrium the space-charge region (on the low-doped side) is essentially depleted of mobile charge carriers. Therefore at all values of reverse biasing voltage the asymmetrical abrupt p-n junction satisfies this particular requirement of the differential capacitance technique, regardless of the doping level of the material under investigation. In contrast, the asymmetical abrupt p-n junction does not exhibit a space-charge region that terminates in a discontinuous fashion. For this reason, questions arise concerning the precise location at which the differential capacitance of this type of junction, in combination with Eq. (7), defines the majority carrier density within semiconductor material.

Questions arising from a lack of abruptness in the spacecharge layer edge, can be answered by returning to Shockley's depletion layer theory for the electrical capacitance of an abrupt asymmetrical p—n junction. ¹⁵ In Shockley's analysis of this problem, approximate methods were used to establish a location for the space-charge layer edge; these approximate methods are well known and will not be repeated here. Thereafter Shockley used this approximate location, in conjunction with Eq. (5), to mathematically establish the junction capacitance; the validity of this approximation has been proved in many experiments using abrupt p—n junctions.

Throughout this investigation, the Shockley depletion layer theory for junction capacitance has remained a valid approximation. In differential capacitance measurements, if the test junction space-charge region is well depleted of mobile charge carriers, the measured junction capacitance arises from the introduction (or removal) of mobile charge carriers from the space-charge layer edge. When this type of junction is used to determine the majority carrier (or impurity) distribution in a semiconductor [by using differential capacitance measurements in conjunction with Eq. (8)], the specific distance from the test junction is given by Eq. (5); this equation establishes the width of an equivalent parallel plane capacitor. If, instead, the test junction spacecharge region is not well depleted of mobile charge carriers (a situation of this kind can occur in a Schottky rectifier), both the carrier density implied by Eq. (8) and the distance implied by Eq. (5) will be in error.

Figure 2 illustrates the calculated space-charge distribution for a Schottky barrier throughout a range of barrier

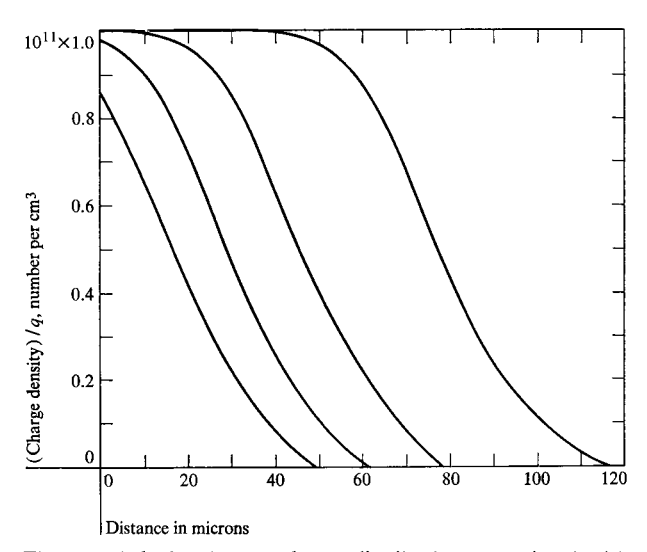


Figure 2 Calculated space-charge distributions associated with a Schottky barrier type of rectifying contact (silicon).

voltages; this computation (Fig. 2) is based upon an impurity atom density of 10^{11} atoms/cm³. In Fig. 2 the space-charge layer does not become suitably depleted of mobile charge carriers until the junction voltage is sufficient to result in a space-charge layer width of approximately $80~\mu$. At small values of junction voltage the differential capacitance of a Schottky barrier can therefore result from changes in electrostatic charge throughout the entire space-charge region, rather than from the edge of this region. Therefore the Schottky barrier sometimes will introduce a substantial error in the inferred impurity atom distribution arising from a series of differential capacitance measurements.

Figure 2 shows that the Schottky barrier does not eliminate a basic difficulty of the abrupt p-n junction: the Schottky barrier must be located a sufficient distance from the region under investigation to assure mobile carrier depletion within the space-charge layer.

The high-low semiconductor junction

Important to the differential capacitance measurement are the physical mechanisms associated with the high-low junction.^{17–21} In most practical situations this measurement is used in an investigation of semiconductor material of homogeneous conductivity type that is known to contain a high-low junction (a region of high conductivity and a region of low conductivity); it is only the detailed impurity atom distribution that is unknown. For this reason the present discussion outlines some properties of a high-low junction that are important in an application of the differential capacitance technique.

It is emphasized that the present discussion is not intended to provide a rigorous and detailed outline of the

physical properties of a high-low junction. The information presented here has been taken from an investigation of high-low junction theory now under way.

Both thermal diffusion and drift contribute to the transport of mobile charge carriers within an impurity semiconductor. If we assume these mobile charge carriers are electrons, the electric current density arising from these transport mechanisms is given by

$$J_n = q D_n \frac{dn}{dx} - q \mu_n n \frac{d\Psi}{dx} \,. \tag{9}$$

For simplicity we shall assume the semiconductor material is n-type and sufficiently extrinsic so that little error is introduced by neglecting minority carriers (holes).

In a high-low junction at equilibrium, the electric current is zero everywhere, and the diffusion and drift components in Eq. (9) are therefore of equal magnitude but in opposite directions. From (9) we obtain for this situation.

$$E(x) = -\frac{d\Psi}{dx} = -\frac{kT}{q} \frac{1}{n(x)} \frac{dn}{dx}.$$
 (10)

Equation (10) establishes the electric field necessary to maintain an electric current of zero in n-type semiconductor material containing local variations in mobile electron density. Because the distribution of mobile electrons is not necessarily known, it is traditional to assume charge neutrality and thereby relate the mobile electron density to the ionized impurity atom density [n(x) = N(x)],

$$E(x) = -\frac{kT}{q} \frac{1}{N(x)} \frac{dN(x)}{dx}.$$
 (11)

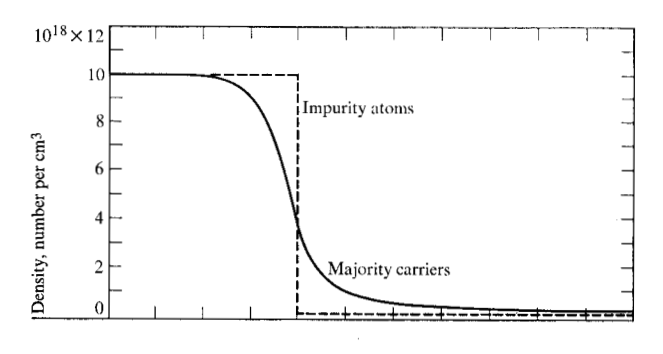
The applicability of this charge-neutral solution (11) is not directly dependent upon the magnitude of the built-in electric field but, instead, upon the rate at which this field is changing. From Poisson's equation,

$$\frac{d^2\Psi}{dx^2} = -\frac{q}{\kappa\epsilon_0} \left[N(x) - n(x) + p(x) \right], \tag{12}$$

the electrostatic charge within a region of semiconductor material governs the rate of change of an electric field within the region under consideration. For this reason it is sometimes incorrect to assume charge neutrality in semiconductor material containing a non-zero impurity atom gradient. Likewise, it is sometimes incorrect to assume that material containing an impurity atom gradient of zero is free of electrostatic charge, and hence free of a built-in electric field.

For example, semiconductor material containing a discontinuous change of impurity atom density (frequently called an abrupt high-low junction) exhibits an electrostatic double-layer of the type attributable to a p-n junction. Figure 3 illustrates the impurity atom distribution, the electron distribution, and the electrostatic charge distribution due to an abrupt transition from 10^{16} to 10^{18}

403



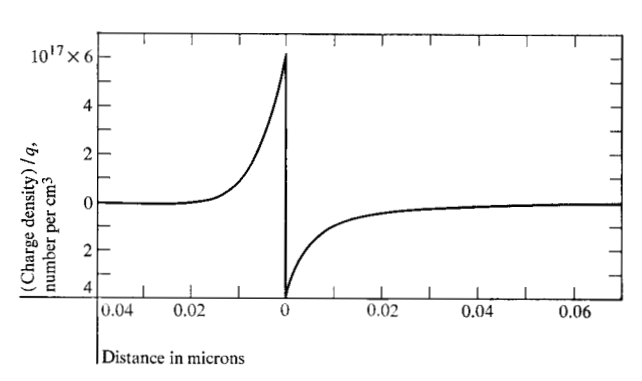
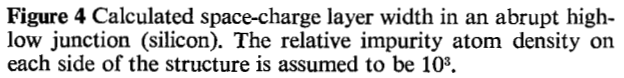
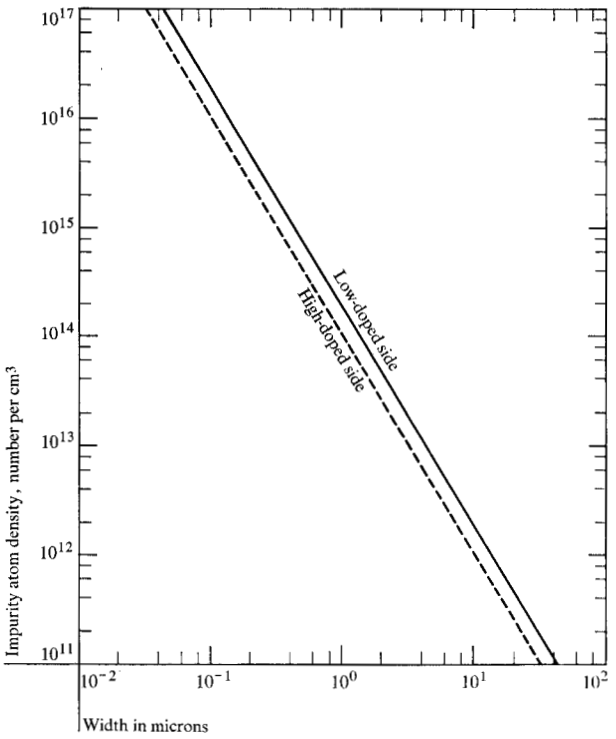


Figure 3 Calculated space-charge characteristics of an abrupt high-low semiconductor junction (silicon).





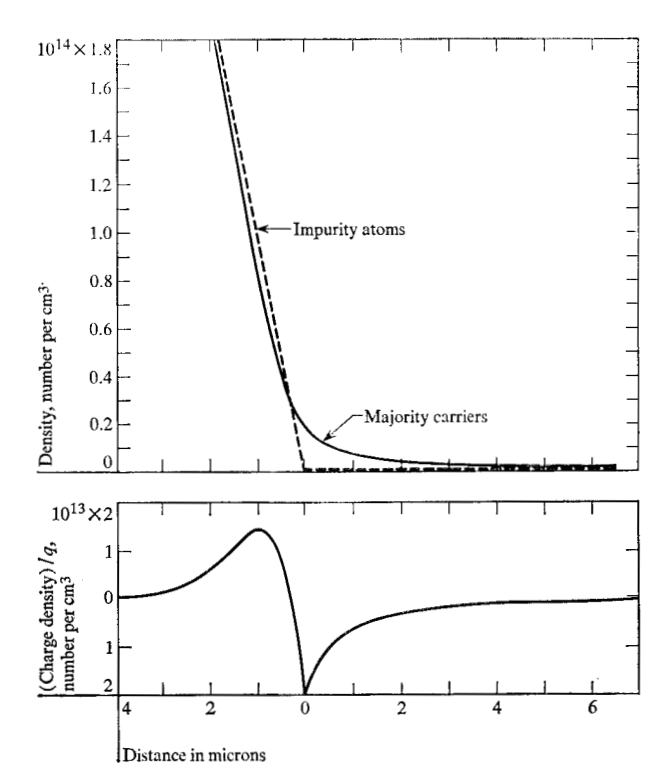


Figure 5 Calculated space-charge characteristics of semiconductor material containing a discontinuous impurity atom gradient (silicon).

atoms/cm³. This illustration was obtained from a detailed numerical solution of Eqs. (1).

Although the electrostatic double-layer associated with a high-low junction is similar to that obtained in a p-n junction, fundamental differences can be observed between these structures. For example, the high-low junction contains a region on the high-doped side that is partially depleted of mobile charge carriers, and a region on the low-doped side that contains an accumulation of mobile charge carriers. Majority carrier accumulation is not observed within the space-charge layer of p-n junctions; in an asymmetrical abrupt p-n junction, the low-doped side contains an electrostatic charge that results from majority carrier depletion.*

Figure 4 illustrates the theoretical space-charge layer width for the abrupt high-low semiconductor junction at potential equilibrium. This illustration results from a series of computer calculations for high-low junctions throughout a wide range of impurity atom densities; the calculations shown in Fig. 4 are based upon an assumed ratio of 10³ for the impurity atom densities on the two sides of the structure. In conjunction with this investigation of the differential capacitance measurement, the space-charge layer edges

[•] This statement neglects minority carrier accumulation that takes place within the low-doped space-charge layer of an asymmetrical abrupt p-n junction; such accumulation has little influence upon the present discussion.

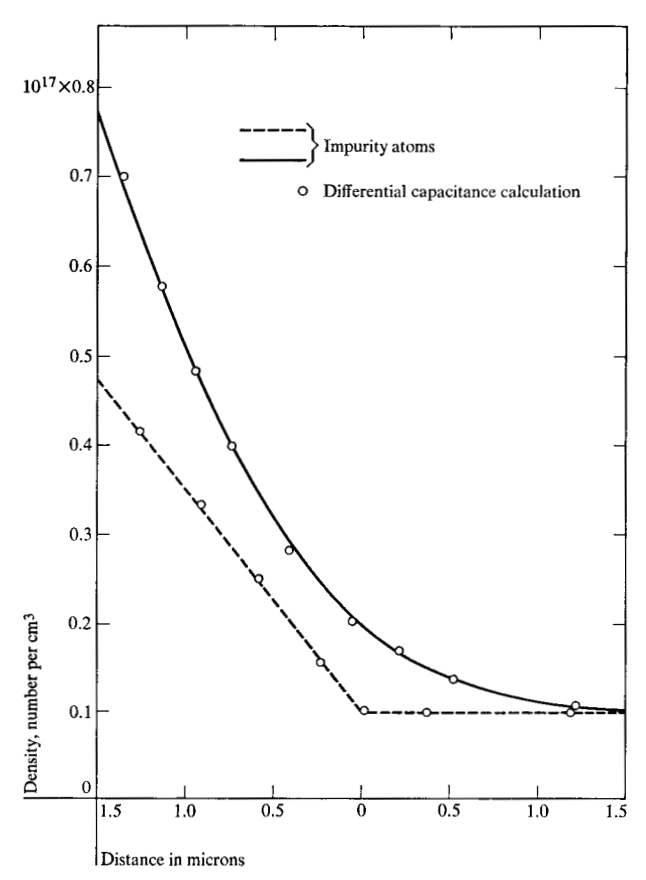


Figure 6 A comparison between the impurity atom distributions in the analytical model (Fig. 1) and those inferred from differential capacitance calculations.

of a high-low junction have been defined as those locations where the space-charge density is either 10% above or below the density of ionized impurity atoms within the semiconductor material.

Another situation leading to an electrostatic charge is the abrupt termination of a linearly-graded impurity distribution into a region of constant doping, Fig. 5. From Eq. (10), a region of constant impurity atom gradient would be expected to produce a condition of near charge neutrality, because only a small change is obtained in the resulting electric field; this small change of electric field is a consequence of variations in the density of impurity atoms N(x). In contrast, a substantial electrostatic charge will be observed at any location where the impurity atom gradient is discontinuously reduced to zero; this charge is a consequence of a built-in electric field that must be returned to zero. From Poisson's equation, an accumulation of majority carriers is required to reduce to zero the electric field arising from the impurity atom gradient, and these majority carriers are taken from the region containing the impurity atom gradient.

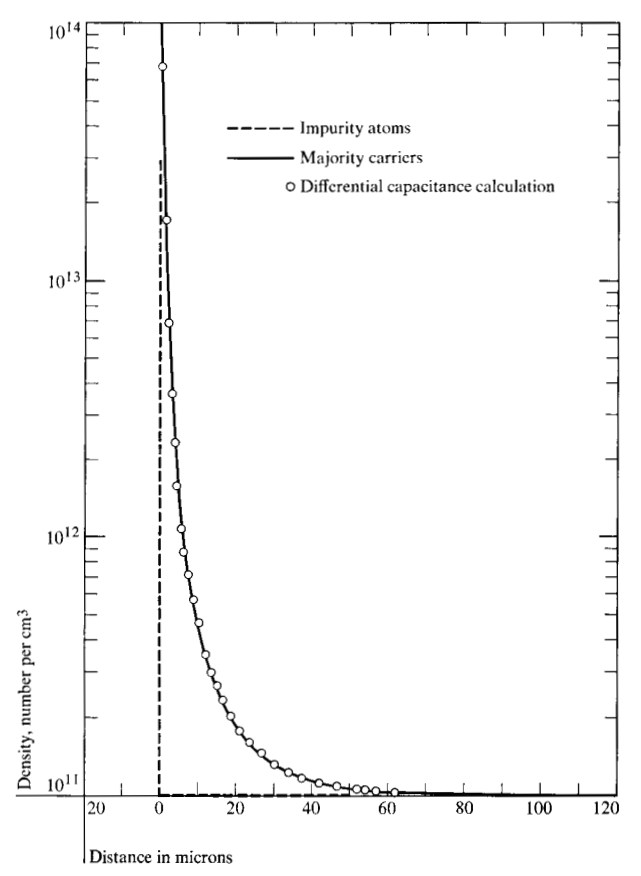


Figure 7 Calculated characteristics for the low-doped side of an abrupt high-low junction (silicon). This figure compares the impurity atom distribution used in the model of Fig. 1, the resulting majority carrier distribution and the profile inferred from differential capacitance calculations.

Analysis

To demonstrate the computational method used in this investigation, Fig. 6 illustrates two different impurity atom distributions that were assumed within the analytical model (Fig. 1) and, in addition, the impurity atom distributions inferred from differential capacitance calculations for the Schottky barrier type of rectifying contact. For all practical purposes, in these examples the differential capacitance technique provides an accurate method for establishing the impurity atom distribution in semiconductor material; the impurity distributions shown in Fig. 6 produce a negligible electrostatic charge and hence n(x) = N(x).

Next, let us consider a situation in which the differential capacitance method is not applicable. Figure 7 illustrates both the assumed impurity atom distribution and the distribution inferred from differential capacitance calculations, applying the same computational methods as were used in the calculations for Fig. 6. In this example (Fig. 7), the semiconductor material is assumed to contain a high-low junction (10¹⁶ to 10¹¹ atoms/cm³) and the differential capacitance calculation is taken from the low

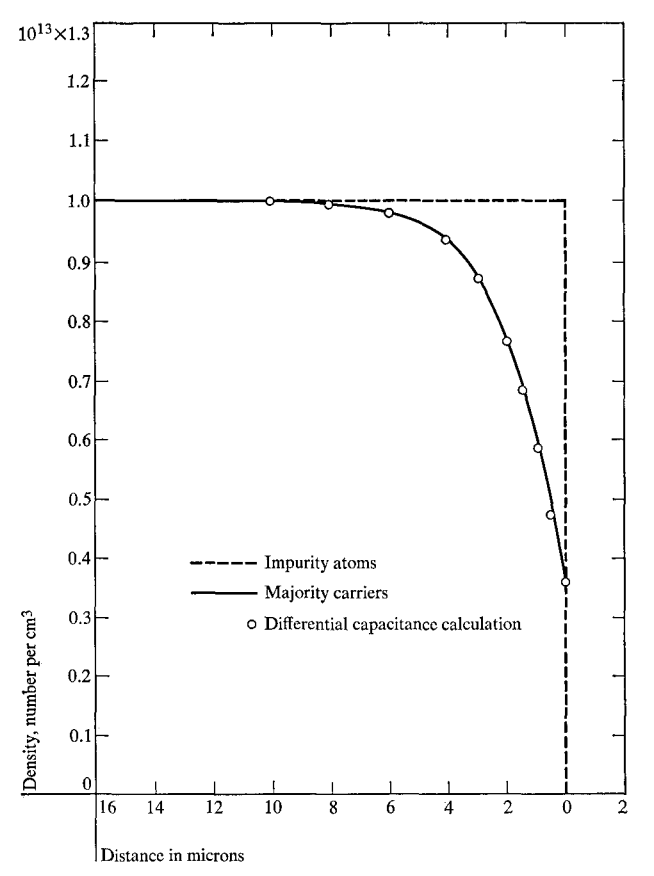
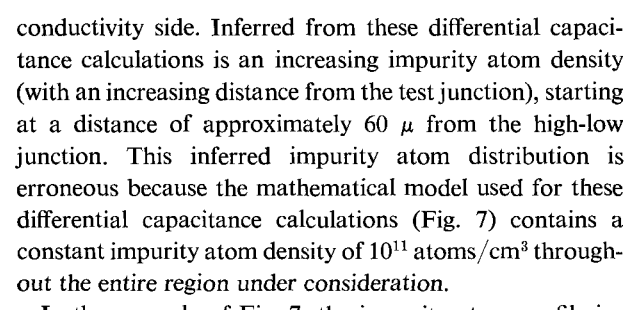


Figure 8 Calculated characteristics for the high-doped side of an abrupt high-low junction (silicon). This figure compares the impurity atom distribution used in the model of Fig. 1, the resulting majority carrier distribution and the profile inferred from differential capacitance calculations.



In the example of Fig. 7, the impurity atom profile inferred by these differential capacitance calculations is quantitatively equal to the mobile carrier distribution within the space-charge region of the particular high-low junction under consideration. This conclusion has been computationally verified for numerous types of high-low semiconductor junctions and for numerous abrupt high-low junctions containing a wide range of impurity atom densities on each side of the structure. Furthermore this conclusion is consistent with Eq. (8), which is applicable to regions of semiconductor material not exhibiting charge neutrality.

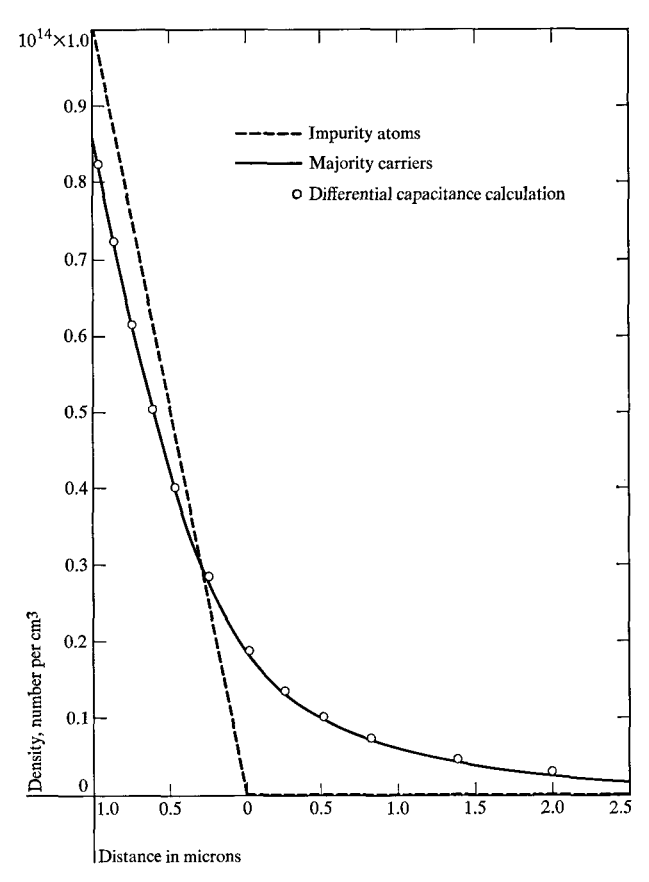


Figure 9 A comparison between the impurity atom distributions assumed in the analytical model (Fig. 1) and the distribution inferred from differential capacitance calculations.

In contrast with the calculations shown in Fig. 7, Fig. 8 illustrates the differential capacitance inferred profile on the high-conductivity side of an abrupt high-low semiconductor junction. The results of this calculation are consistent with both Eq. (8) and the computations illustrated in Fig. 3. The differential capacitance inferred impurity atom density (Fig. 8) starts to decrease at a distance of 8.0 μ from the semiconductor junction; the actual impurity atom density within this model is constant, being maintained at 10^{13} atoms/cm³. Furthermore, this inferred impurity atom density is in quantitative agreement with the calculated mobile electron density within this region of the device.

In Fig. 9, as in Figs. 7 and 8, the impurity atom distribution inferred from the differential capacitance calculations is quantitatively equal to the distribution of mobile charge carriers associated with the electrostatic double-layer of the structure. In this example (Fig. 9), the double-layer is attributable to a discontinuous change of impurity atom gradient within the mathematical model.

Figures 7 and 8 illustrate that the error associated with

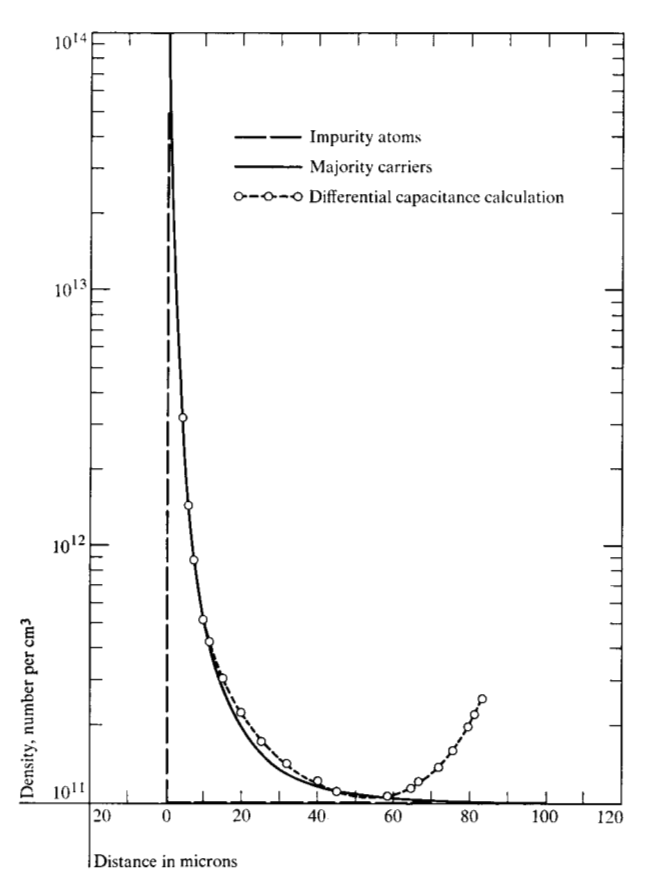


Figure 10 Calculated characteristics for the low-doped side of an abrupt high-low junction (silicon). This figure compares the impurity atom distribution used in the model of Fig. 1, the resulting majority carrier distribution and the profile inferred from differential capacitance calculation. The test junction was located $100~\mu$ from the high-low junction.

a differential capacitance inferred impurity atom profile is directly related to the electrostatic charge existent within the region under investigation. In the vicinity of a high-low junction, differential capacitance calculations can indicate an impurity atom density that is either greater (low-doped side) or smaller (high-doped side) than the one actually present. A further illustration of this error is shown in Fig. 9, where differential capacitance measurements would indicate an impurity atom density that is too large in one region and too small in another region of the same structure.

The computations shown in Figs. 7, 8 and 9 illustrate the errors associated with the differential capacitance technique when applied to semiconductor material containing an electrostatic charge. In a practical situation, it must be assumed that the impurity atom distribution is unknown, and therefore one cannot determine the electrostatic charge distribution in a given sample of silicon. One approach to this problem is to assume that the material under investigation contains an abrupt high-low junction, and from Fig. 4 determine the space-charge width on each side of this assumed junction. From this width, the maximum error

associated with an actual differential capacitance experiment can be estimated.

Aside from the error arising when $n(x) \neq N(x)$, it has also been stated that incomplete mobile carrier depletion from the test junction space-charge layer represents another source of error. To eliminate this difficulty the calculations shown in Figs. 7, 8 and 9 were based upon an assumed semiconductor thickness of about 200 μ on the low-doped side. In contrast, Fig. 10 illustrates a recomputation of Fig. 7 except that the thickness of the semiconductor material is assumed to be only 100 μ on the low-doped side.

In Fig. 10 two sources of error are exhibited by the impurity distribution inferred from these differential capacitance calculations. First, at small values of applied voltage (small penetration of the junction space-charge layer) the test junction space-charge layer is not adequately depleted of mobile charge carriers; this error is eliminated at a space-charge layer penetration of about 90 μ from the semiconductor surface. Second, the high-low junction introduces the same type of electrostatic charge as that shown in Figs. 3 and 7 and therefore, after suitable penetration of the test junction space-charge layer, the differential capacitance calculation establishes the distribution of mobile electrons, not the distribution of impurity atoms.

The authors recognize that the foregoing computational examples (Figs. 7–10) are based upon impurity atom densities not frequently used in the fabrication of semiconductor devices. The small impurity atom densities used in these examples are intended to emphasize the errors associated with the differential capacitance technique rather than to provide quantitative information for any specific semiconductor doping level. Furthermore, these examples suggest possible errors in published work on the evaluation of doping profiles introduced into semiconductor material by ion implantation.

It has been reported that 20 kV implantations on high-resistivity silicon (20 to 50 k Ω -cm) resulted in a deep penetration of donors;²¹ this is suggested to reflect a basically different mechanism determining the distribution of implanted ions. Furthermore it is reported that the profiles upon which this conclusion is based were determined by differential capacitance techniques (using a Schottky barrier) upon silicon samples approximately 100 μ in width (or less). It is for this reason that Fig. 10 is presented here.

Figure 11 presents a comparison between the mobile carrier distribution inferred from differential capacitance calculations and Fig. 1 from the referenced publication on ion implantation. ²¹ In these calculations (Fig. 11), an abrupt high-low junction was assumed in the mathematical model, and the high-doped side of this junction was maintained at the reference doping level used in these implantation experiments (10¹⁶ atoms/cm³). On the low-doped side of this mathematical model, the impurity atom density was selected to obtain adequate agreement between experiment

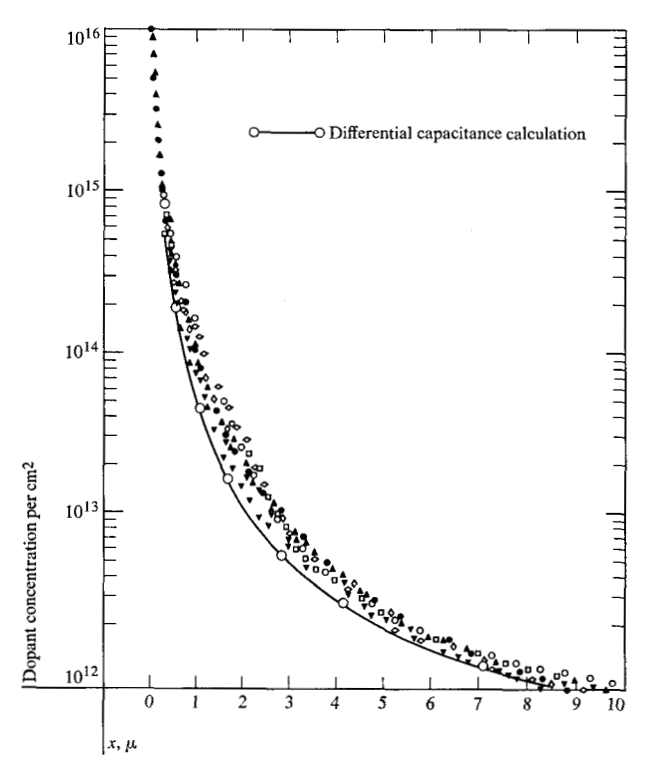


Figure 11 A comparison between the measured doping profile arising from ion implantation experiments (Fig. 1 of Ref. 20) and the results of differential capacitance calculations for an abrupt high-low junction.

and the theory presented here. This agreement was obtained with an assumed impurity atom density of 4.0×10^{11} atoms/cm³, which is substantially the same as the published value (about 1.0 to 2.0×10^{11} atoms/cm³). It should be noted that the experimental data shown in Fig. 11 were reported to have been obtained upon silicon slices with thickness ranging between 25 and 120 μ ; the computed results shown in Fig. 11 are based upon an assumed slice thickness of 100μ .

From this mathematical investigation, and from Fig. 11, it is suggested that the inferred deep donor penetration due to ion implantation is a consequence of errors attributable to the differential capacitance measurement. Figure 11 suggests that this implantation is sufficiently shallow to be considered an abrupt high-low junction, and that the differential capacitance measurement establishes the mobile carrier distribution associated with this type of structure, rather than the doping profile. Furthermore Fig. 10 indicates that by using a Schottky barrier in conjunction with a narrow slice of silicon, incomplete depletion of the test junction space-charge layer may be introducing additional errors in the interpretation of the data shown in Fig. 11.

Conclusions

This investigation shows that differential capacitance measurements of an impurity atom profile are applicable only to regions of semiconductor material that are nearly charge-neutral. An analysis of this technique shows that differential capacitance measurements establish the distribution of majority carriers rather than impurity atoms; the two distributions (majority carriers and impurity atoms) are equivalent only in regions exhibiting charge neutrality. Although complete charge neutrality is not likely in semiconductor material containing an inhomogeneous distribution of impurity atoms, little error should result from measurements of material containing an impurity atom density in excess of 10½ atoms/cm³.

Little can be said concerning the applicability of this measurement to material containing a small impurity atom density. If the impurity atom profile were known, calculations could be performed to determine the resulting electrostatic charge distribution; thereby the applicability of differential capacitance measurements could be established. In most practical situations the impurity atom distribution is unknown and, furthermore, a detailed knowledge of the impurity atom distribution would eliminate any need for performing these differential capacitance measurements. At this time there is no known method whereby information obtained from differential capacitance measurements of low-doped material could be used to establish the impurity atom distribution. For this reason, differential capacitance inferred impurity atom distributions should be placed in question when the doping level is below approximately 10^{16} atoms/cm³.

A possible consequence of this situation is demonstrated by comparing the measured and calculated doping profiles arising from ion implantation experiments into high-resistivity silicon (Fig. 11). The measured doping profile indicates a penetration depth far in excess of existing theoretical information on ion implantation. In contrast, calculations indicate that the measured doping profile is in substantial agreement with the theoretical electron distribution for an abrupt high-low semiconductor junction. It is therefore suggested that the observation of deep donor penetration in these experiments is a consequence of errors attributable to the differential capacitance measurement.

Acknowledgments

The authors wish to thank Dr. D. Young for his continued interest and his support of this analytical effort. They also thank Dr. R. R. O'Brien for many valuable suggestions during the course of this work.

References

- C. O. Thomas, D. Kahng, and R. C. Manz, J. Electrochem. Soc. 109, 1055 (1962).
- N. I. Meyer and T. Guldbrandsen, Proc. IEEE 51, 1631 (1963).

- 3. I. Amron, Electrochem. Tech. 2, 337 (1964).
- 4. I. Amron, Electrochem. Tech. 5, 94 (1967).
- 5. W. Van Roosbroeck, Bell System Tech. J. 29, 560 (1950).
- 6. W. Shockley and W. T. Read, Jr., Phys. Rev. 87, 835 (1952).
- R. V. Southwell, Relaxation Methods in Engineering Science, Oxford University Press, London, 1940.
- R. V. Southwell, Introduction to the Theory of Elasticity, Oxford University Press, London, 1941.
- R. V. Southwell, Relaxation Methods in Theoretical Physics, Vol. I, Oxford University Press, London, 1946.
- R. V. Southwell, Relaxation Methods in Theoretical Physics, Vol. II, Oxford University Press, London, 1956).
- G. E. Forsythe and W. R. Wasow, Finite-Difference Methods for Partial Differential Equations, John Wiley & Sons, New York, 1960.
- 12. H. K. Henisch, *Rectifying Semiconductor Contacts*, Oxford University Press, London, 1957.
- 13. W. R. Smythe, Static and Dynamic Electricity, McGraw-Hill Book Co., Inc., New York, 1950.

- 14. G. P. Harnwell, *Principles of Electricity and Electromagnetism*, McGraw-Hill Book Co., Inc., New York, 1938.
- 15. W. Shockley, Bell System Tech. J. 28, 435 (1949).
- 16. J. J. Sparkes, J. Electronics and Control 16, 153 (1964).
- 17. J. B. Arthur et al., Proc. Phys. Soc. (London) B68, 43 (1955).
- J. B. Arthur, A. F. Gibson, and J. B. Gunn, *Proc. Phys. Soc. (London)* B69, 697 (1956).
- J. B. Arthur, A. F. Gibson, and J. B. Gunn, *Proc. Roy. Soc.* (*London*) B69, 705 (1956).
- 20. J. B. Gunn, J. Electronics and Control 4, 17 (1958).
- 21. R. W. Lade and A. G. Jordan, *J. Electronics and Control* 13, 23 (1962).
- 22. R. W. Bower, R. Baron, J. W. Mayer, and O. J. Marsh, *Appl. Phys. Letters* **9**, 203 (1966).

Received April 30, 1968.